Proceedings of ASME Turbo Expo 2011
GT2011
June 6-10, 2011, Vancouver, British Columbia, Canada

GT2011-45735

THE INFLUENCE OF LEADING EDGE DIAMETER ON STAGNATION REGION HEAT TRANSFER AUGMENTATION INCLUDING EFFECTS OF TURBULENCE LEVEL, SCALE, AND REYNOLDS NUMBER

P. Gandavarapu and F.E. Ames
Mechanical Engineering Department
University of North Dakota
Grand Forks, ND 58202

ABSTRACT

Stagnation region heat transfer measurements have been acquired on two large cylindrical leading edge test surfaces having a four to one range in leading edge diameter. Heat transfer measurements have been acquired for six turbulence conditions including three grid conditions, two aero-combustor conditions, and a low turbulence condition. The data have been run over an eight to one range in Reynolds numbers for each test surface with Reynolds numbers ranging from 62,500 to 500,000 for the large leading edge and 15,625 to 125,000 for the smaller leading edge. The data show augmentation levels of up to 110% in the stagnation region for the large leading edge. However, the heat transfer results for the large cylindrical leading edge do not appear to infer a significant level of turbulence intensification in the stagnation region. The smaller cylindrical leading edge shows more consistency with earlier stagnation region heat transfer results correlated on the TRL parameter. These results indicate that the intensification of approaching turbulence is more prevalent with the more rapid straining of the smaller leading edge. The downstream regions of both test surfaces continue to accelerate the flow but at a much lower rate than the leading edge. Bypass transition occurs in these regions providing a useful set of data to ground the prediction of transition onset and length over a wide range of Reynolds numbers and turbulence intensity and scales.

INTRODUCTION

Cooling the stagnation region of a turbine airfoil has always been an important consideration in hot section design. Depending on the performance and operation considerations of the engine as well as the fuel and air quality the leading edge of turbine airfoils can either be internally cooled or rely on showerhead type film cooling arrays. New land based gas turbines are becoming larger producing higher chord and leading edge Reynolds numbers. At high Reynolds numbers stagnation heat transfer levels on a vane are expected to be much lower than the turbulent regions of flow found over the suction surface and much of the pressure surface. However, current land based machines have leading edge Reynolds numbers exceeding 300,000. Depending on the combustion system inlet turbulence levels could be 20% or higher. At the same time industry trends show larger leading edge diameters in first vanes. Currently, designers simply do not have a reliable data base at the most aggressive stagnation region conditions expected for land based gas turbines. The present study has been designed to extend the parameter range for stagnation region heat transfer to encompass the range expected for modern engines. This research will also investigate the effects of larger stagnation regions on heat transfer augmentation due to the response of turbulence in the leading edge strain field. The experimental data also include heat transfer distributions downstream from the stagnation region which show transitional and fully turbulent flow behavior.

NOMENCLATURE

A	disturbance amplitude [22]
C	vane true chord length, m
c_P	specific heat at constant pressure, J/kg/K
D	leading edge diameter, m
h	heat transfer coefficient, W/m^2/K
Δh_t	turbulent enhancement to heat transfer coefficient, W/m^2/K
k	thermal conductivity, W/m/K
Lu	energy scale, $Lu = 1.5\, |u'|^3/\varepsilon$
Nu_D	diameter Nusselt number, $Nu = hD/k$
Pr	Prandtl number, $Pr = \nu/\alpha$
Re_D	Reynolds number based on diameter and approach velocity
T	temperature, K
Tu	turbulence level, $Tu = |u'|/U_\infty$
U_∞	freestream velocity, m/s
u', |u'|	streamwise component rms fluctuation velocity, m/s
V_{APP}	approach velocity to cylinder
X	distance, streamwise direction, m
Y	distance, normal direction, m

Greek Letter Symbols

α	thermal diffusivity, m^2/s, $\alpha = k/\rho c_P$
ε	turbulent dissipation rate, m^2/s^3
ε_M	eddy diffusivity for momentum, m^2/s
λ	disturbance wavelength [22], m

Λ_X longitudinal integral scale of u' fluctuation
ν kinematic viscosity, m^2/s
ρ fluid density, mass per unit of volume, kg/m^3

Subscripts

∞ evaluated in the free stream

BACKGROUND

Influence of Turbulence on Stagnation Region Heat Transfer. Turbulence is known to augment stagnation region heat transfer. Zapp [1] was an early investigator on the influence of turbulence on cylindrical heat transfer. He generated turbulence levels of 3.0% and 11.5% using grids and reported heat transfer increases as high as 68%. Smith and Kuethe [2] investigated laminar heat transfer on a flat plate and a circular cylinder subjected to round rod square mesh grid generated turbulence. They suggested that the eddy diffusivity across the laminar boundary layer was proportional to the streamwise fluctuation velocity times the wall normal distance ($\varepsilon_M \propto$ Tu U_∞ y). They found an approximately linear relationship between $Nu_D/Re_D^{1/2}$ and a parameter $TuRe_D^{1/2}$ they developed to correlate their results. Smith and Kuethe's correlating parameter, $TuRe_D^{1/2}$, has previously been used as the basis to fit data from a range of investigations. Examples of investigators which used $TuRe_D^{1/2}$ to develop correlations include Kestin and Wood [3] and Lowery and Vachon [4]. Mehendale and Han [5] studied grid generated turbulence on stagnation region heat transfer. They used two square bar square mesh grids and an innovative jet grid to generate turbulence. They compared their results to Lowery and Vachon's correlation and generally found their data were slightly underpredicted.

Response of Turbulence in Stagnation Region Strain Fields. Hunt [6] used rapid distortion theory to predict the response of turbulence in the presence of a circular cylinder in crossflow. He performed calculations for spectra for the limiting cases of very small scales and very large scales. His results suggest that relatively small scales are intensified by the stagnation region strain field and that relatively large scales are attenuated in a manner similar to the mean flow. Britter, Hunt, and Mumford [7] experimentally investigated the response of turbulence with a range of scales to a flow field around a cylinder. Their turbulent length scale to diameter ratio (Λ_X/D) ranged from 0.35 to 10. Their data generally supported Hunt's predictions. They determined the response of spectra approaching a cylinder and found the amplification of relatively high wave number spectra by the cylindrical strain field and the blocking of relatively low wavenumber spectra by the cylinder's surface.

Instabilities of Velocity Variations. Rigby and Van Fossen [8] numerically studied the influence of spanwise variations of freestream velocity on cylindrical stagnation region heat transfer. They found the vorticity introduced by the spanwise variations amplified as it approached the stagnation region due to vortex stretching. They found this mechanism can cause periodic arrays of structures similar to horseshoe vortices, which produce a substantial increase in the spanwise averaged heat transfer rate.

Influence of Turbulence Scale. The influence of turbulent scale on heat transfer has previously been considered as an important variable. Kestin [9] suggested that an implicit assumption that figured into many early heat transfer studies was that the turbulent scale was sufficiently small in comparison with the dimensions of the body. Ames and Moffat [10] studied the influence of high intensity large scale turbulence on cylindrical stagnation region heat transfer. Their data fell well below Kestin and Wood's [3] correlation and grouped based on cylinder diameter for a given turbulence generator. They developed a simple spectral model based on the work of Hunt [6] and Britter, Hunt, and Mumford [7] which accounted for the intensification of high wavenumber spectra due to the straining and the blocking of low wavenumber spectra due to the proximity to the surface. They used the spectral model to develop a simple eddy diffusivity model. They developed a correlating parameter for stagnation region heat transfer based on the eddy diffusivity model using scaling derived from the turbulent heat flux equation. Ames, et al. [10, 11, 12, 13, 14] have correlated a range of stagnation region heat transfer data with the TRL parameter [Tu $Re_D^{5/12}$ $(Lu/D)^{-1/3}$] and suggested that a good engineering approximation to heat transfer augmentation in a stagnation region is $Nu/Nu_0 = 1 + 0.04*TRL$. Van Fossen, Simoneau, and Ching [15] studied the influence of turbulence parameters, Reynolds number, and body shape on stagnation region heat transfer. They generated turbulence with four square bar square mesh grids and one array of parallel wires and estimated the turbulent time scale by fitting the autocorrelation in time to $R(t) = e^{-C\tau \cdot \tau}$. Their length scale to diameter ratios ranged from 0.05 to 0.3 and their data collected on Smith and Kuethe's [2] parameter as a function of grid size. They developed an empirical correlation for all their body shapes which suggested that $Nu/Nu_0 = 1 + 0.00851\,[Tu\, Re_D^{0.8}\, (\Lambda_X/D)^{-0.574}]^{1/2}$. Later, Van Fossen and Bunker [16] measured stagnation region heat transfer downstream from a DLN can combustor with a turbulence level of 28% finding an augmentation level of 77%. The DLN data was significantly underpredicted by Van Fossen's parameter and slightly over predicted by the TRL parameter.

Dullenkopf and Mayle [17] proposed a different correlation for stagnation region heat transfer which they also suggested would be applicable to correlating turbulent augmentation of laminar heat transfer on the pressure surface of a turbine airfoil. They included Ames and Moffat's [10] data in the development of their correlation. They based their correlation on an effective turbulence level, Tu_λ, where Tu_λ is a function of turbulence intensity (Tu), diameter Reynolds number (Re_D), the ratio of the macro scale of turbulence to diameter (L/D) and a constant a_1 related to the local strain rate. However, for relatively large scale turbulence, their effective turbulence parameter can be shown to reduce to a function of Tu $Re_D^{1/3}$ $(Lu/D)^{-1/3}$. Ames [11] and Ames et al. [12, 13] studied heat transfer on the stagnation regions and laminar pressure surfaces of vanes. They suggested that while heat transfer augmentation in the stagnation region appeared to correlate on the TRL parameter [Tu $Re_D^{5/12}$ $(Lu/D)^{-1/3}$], augmentation on the pressure surface correlated more closely to [Tu $Re_C^{1/3}$ $(Lu/C)^{-1/3}$]. They suggested that turbulence in the stagnation region was intensified by the strain field. However, even though the relative level of heat transfer augmentation was high, the straining of turbulence along the pressure surface had no discernable effect on heat transfer augmentation. Oo and Ching [18] investigated the influence of vortical structures in the flow by generating turbulence with uni-planar round rod grids perpendicular and parallel to the stagnation line. Oo and Ching's data did not correlate well with Van Fossen's correlation and improved significantly when a dimensionless vortex parameter was included. Nix et al. [19], Nix and Diller [20], and Gifford et at. [21] looked at the coherence between turbulent fluctuations and transient heat flux excursions to stagnation region heat transfer. Nix [19] suggested the increase in stagnation region heat transfer could be correlated based on the characteristic time of the event, Λ_X/u'_{RMS} or $\Delta h_t = k/[\pi\alpha\Lambda_X/u'_{RMS}]^{1/2}$.

Direct Numerial Simulation of Turbulence. Bae, Lele, and Sung [22] analyzed the effect of sinusoidal disturbances on stagnation region heat transfer using direct numerical simulation. Bae et al. imposed a disturbance of wavelength, λ, and relative amplitude, *A*, on the free stream similar to Rigby and Van Fossen [8]. They found three regimes which they called (a) the damping regime where $\lambda/\delta < 2.7$, (b) the attached amplifying regime where $2.7 < \lambda/\delta < 5.3$ and (c) the detached amplifying regime where $\lambda/\delta > 5.3$. Here δ is the boundary layer thickness for the undisturbed flow. In the damping regime, disturbances were damped and heat transfer augmentation was lower. In the attached amplifying regime, the streamwise vorticity was attached to the wall and heat transfer, for a given Reynolds number and amplitude, was maximized. In the detached amplifying regime, the streamwise vorticity was detached from the wall and the heat transfer augmentation decreased with increasing wavelength. Results from the attached and detached amplifying regimes correlated well using the TRL [10, 11] correlation. Note that Bae's disturbances had a single wavelength and orientation, while turbulence has a range of eddy sizes and orientations.

Present Viewpoint. The augmentation of stagnation region heat transfer due to flow field turbulence is a scientifically interesting problem with high relevance to gas turbine design. Different investigators have studied this problem and have attempted to rationalize results from a range of different perspectives including empirical, turbulent spectrum based, coherent structure, and numerical. The main focus of this present paper is to systematically expand the parameter range into higher Reynolds numbers by using larger diameter cylinders. Stagnation region heat transfer has been studied using these large cylinders with high turbulence levels over a range of turbulent scales. The present author's have chosen to favor the perspective of references [10-14] in analyzing and reporting these results. However, the authors are willing to make this comprehensive data set available to other investigators in this area.

EXPERIMENTAL APPROACH

The experimental measurements were all acquired in a relatively large scale low speed wind tunnel facility. Two large cylindrical leading edge test surfaces were used to acquire the stagnation region and downstream surface heat transfer measurements reported in this paper. Two grids and a mock aero-combustor turbulence generator were used to generate 5 inlet turbulence conditions for this study in addition to a baseline low turbulence condition.

Low Speed Wind Tunnel. The relatively large scale low speed wind tunnel facility used to acquire surface heat transfer measurements is shown in **Figure 1**. The inlet to the wind tunnel consists of a filter box with eight large high-efficiency commercial air filters. The filter box is connected to the inlet of a centrifugal blower. A 45 kW motor powers the blower which is controlled using a variable frequency drive. The blower is capable of providing 6.6 m^3/s of air with a static pressure rise of 5000 Pa. The blower directs the air into a two stage multivane diffuser which in turn delivers the air to a heat exchanger. The water cooled heat exchanger is responsible for removing the thermal energy from the air to keep the inlet air temperature constant for the steady state heat transfer measurements. A rectangular spool delivers the air from a heat exchanger to a flow conditioning section. The flow conditioning section consists of four nylon screens spaced at 8 cm. The flow conditioning section connects to a nozzle with a 3.6 to 1 area ratio contraction. The contraction connects to a 0.254 m wide by 1.27 m high rectangular cross-section. The 1.143 m long test section is used to hold one of the two cylindrical leading edge test surfaces.

Turbulence Generation. A total of six inlet turbulence conditions were generated including a low turbulence baseline condition. The low turbulence baseline condition was developed using the combination of the screen box and the nozzle with a 3.6 to 1 area ratio contraction, generating a turbulence intensity of around 0.7%. Two grids with a two to one variation in mesh spacing were also used to generate turbulence. The small grid used a 0.635 cm square bar on a 3.175 cm mesh in a biplanar arrangement with 64% open area. This smaller grid was placed in a rectangular spool 10 and 32 mesh lengths upstream from the cylinder leading edge generating intensities estimated at 9.2% and 3.1% respectively at the measurement plane. A larger grid was also developed with double the bar size (1.27 cm) and double the mesh size (6.35 cm). The larger grid was also placed in the spool 10 mesh lengths upstream from the cylinder leading edge plane and generated an intensity of around 8.5% at the measurement plane. Two levels of large scale high intensity turbulence were also generated using a model aero-combustor shown schematically in **Figure 2**. The model aero-combustor produces recirculation zones in the front of the combustor with the slots in the back panel and the first row of plunged holes. The second row of plunged holes acts similar to dilution jets. The model aero-combustor generates large scale ($Lu \cong 7$ cm) turbulence with an intensity of around 13.5% at the measurement plane 7 cm upstream from the leading edge plane of the test section. A lower level (9.3%) of large scale turbulence is generated by placing the 0.91 m long rectangular spool between the model combustor and the heat transfer test section. The six turbulence conditions generated in this study are presented in **Table 1**. All measurements documented in Table 1 were acquired using a miniature single hotwire powered by constant temperature anemometer. Each determination of velocity, U_∞, turbulence intensity, Tu, integral scale, Λ_X, energy scale, Lu, and dissipation, ε, is statistically well resolved and typically based on the average at several locations in the measurement plane. A more complete description of the typical turbulence measurement and analysis procedure is given in [12]. Note that turbulence intensities used for the TRL parameter were based on the expected decay from the measurement plane to the cylinder leading edge plane.

Heat Transfer Test Surfaces. The heat transfer test surfaces were designed with 0.1016 m and 0.4064 m diameter leading edge surfaces over the first +/- 30°. The remainder of the heat transfer test surface was designed to accelerate the flow smoothly along the surface of the after body. The half profiles of the geometry for the leading edge surfaces are presented in **Figure 3**. The cylindrical leading edge surfaces reside inside a 0.254 m wide by 1.27 m high test surface. The leading edge of the test surfaces are placed 0.127 m downstream from the inlet of the 1.143 m long test section. The predicted free-stream velocity distributions off the surface of the 0.1016 m and 0.4064 m leading edge test surfaces are presented in **Figure 4**. The velocity distributions were determined from surface pressure distributions over the two test surfaces generated using well resolved 2-D FLUENT calculations. The models included the full test section around the cylindrical surface and an equal section upstream. The surface velocity distributions initially show a strong region of constant acceleration over the first 30° of the leading edge cylindrical surface and later the rate of growth of velocity decreases substantially. The cylindrical surfaces are fabricated out of polyisocyanurate foam and are covered with 0.38 mm G10 fiberglass epoxy board. The 0.4064 m cylindrical surface has 47 type K fine wire thermocouples epoxied into the G10 surface while the 0.1016 m cylindrical surface has 63 thermocouples epoxied into its surface. The midspan of the 0.4064 m cylinder initially has streamwise spacings of 2.54 cm near the stagnation region which changes to 5.08 cm spacings away from the cylindrical stagnation region. The other thermocouples have been placed +/- 5.08 cm off span with initial spacings of 5.08 cm moving to 10.16 cm away from the stagnation region. The midspan of the 0.1016 m diameter leading edge surface initially has 0.85 cm spacings near the stagnation line gradually moving to 5.08 cm spacings toward the ends of the test surface. Two rows of off span thermocouples are placed at +/- 5.08 cm from midspan with streamwise spacings which are double the midspan distribution. Each surface is wrapped with a 0.023 mm thick Inconel foil with a nominal area of 100 cm by 25 cm. The Inconel foil is backed with a 0.05 mm thick Kapton sheet which is adhered to the epoxy board surface with high temperature acrylic adhesive. Nominally, the foil covers -0.15 m to +0.85 m from the stagnation line along the cylindrical surface and after body.

The constant heat flux was generated by passing a large DC current through the Inconel foil. The rate of resistance heating was determined by measuring the voltage across and the current through the foil. The current was determined by measuring the voltage across a precision shunt resistor. The net heat flux was determined by subtracting the rate of thermal radiation from the calculated foil heat flux. The heat transfer coefficient was determined by dividing the net heat flux by the heated-wall to adiabatic-wall temperature difference, set at a minimum of at least 4 °C. The local heated wall to adiabatic wall temperature difference was determined from steady state adiabatic-wall and heated-wall temperature distributions referenced to the inlet total temperature. The reported Nusselt numbers were based on the nominal leading edge diameter of the heat transfer surface and the thermal conductivity taken at the inlet total temperature. All data reported in this paper were acquired at low velocities and at low surface to free-stream temperature ratios. At higher velocities and higher temperature ratios the effect of the adiabatic wall to free-stream temperature ratio and surface to free-stream temperature ratio can impact heat transfer rates due to variable properties across the boundary layer and should be considered in applying the reported results.

Baseline Heat Transfer. Low turbulence Nusselt number distributions were acquired in order to provide confidence in the measurement technique and for comparison purposes for the augmented levels of heat transfer with high free stream turbulence. The diameter Nusselt number (Nu_D) for the stagnation region for a cylinder in crossflow can be determined from the Falkner-Skan similarity flow solutions for momentum and energy. Accounting for the influence of Prandtl number for gases, the general solution for stagnation flow is typically given as [23]:

$$Nu_X = 0.57\, Re_X^{0.5}\, Pr^{0.4} \qquad (1)$$

Since the Nusselt number is typically constant near the stagnation region, this solution can be developed in terms of Nu_D by substituting the following relationship for velocity in the vicinity of a stagnation region of a cylinder (see [24]):

$$U_\infty(x) = 3.63\, V_{APP}\, X/D \qquad (2)$$

The classical potential flow solution gives the constant as 4 instead of 3.63. However due to separation on the sides of a cylinder during subcritical flow the value given in equation (2) is better for cylinders in cross flow. Substituting this relationship into equation (1) and using a Prandtl number for air of 0.707 the typical baseline relationship can be described as:

$$Nu_D/Re_D^{0.5} = 0.945 \qquad (3)$$

While the result provided by equation (3) is a constant temperature solution, in a 2-D stagnation region the heat transfer coefficient and thus the surface temperature for the constant heat flux boundary condition is expected to be constant. **Table 2** provides the stagnation region results for $Nu_D/Re_D^{0.5}$ taken at low turbulence with the present heat transfer surfaces with cylindrical leading edges. The results for the 0.1016 m cylindrical leading edge are clearly much lower than this value while the results for the 0.4064 m cylindrical leading edge are noticeably higher. Two complicating issues generally cause difficulties in achieving the stagnation region heat transfer value given by equation (3). One issue is related to the amplification of instabilities described by Rigby and Van Fossen [8]. Also, leading edges on 2-D surfaces other than cylinders in cross flow or flows with significant compressibility will have a constant different from the value (3.63) given in equation (2). Based on 2-D FLUENT calculations, the stagnation region acceleration constants for the smaller and larger heat transfer surfaces with cylindrical leading edges are 3.10 and 4.08 respectively. These accelerations lead to $Nu_D/Re_D^{0.5}$ of 0.873 and 1.002 respectively for the smaller and larger stagnation regions. Remaining differences are likely due to differences between actual and predicted accelerations, amplification of instabilities, and experimental uncertainty.

The surface heat transfer distributions were also compared with STAN7 finite difference boundary layer calculations. **Figure 5** presents distributions of diameter Nusselt number for the 0.1016 m leading edge test surface taken at approach flow diameter Reynolds numbers of 15,625, 31,250, 62,500, and 125,000. Generally, the experimental and predicted distributions compare favorably with typical differences less than 5% over most of the surfaces. However, some differences between experiment and prediction are as large as 10% but are largely explainable by instabilities that can be amplified at the leading edge and which can convect downstream over test surface. **Figure 6** shows comparisons between experimental and predicted Nu_D distributions for leading edge test surface at Reynolds numbers of 62,500, 125,000, 250,000, and 500,000. Due to the four to one difference in leading edge diameter, the approach velocity Reynolds number is four times larger for the big leading edge. Generally, the comparisons between the experimental and predicted distributions of Nu_D are quite good. However, at the highest two Reynolds numbers the experimental heat transfer levels begin to rise above the experimental predictions with the start of transition evident on the downstream surface at the largest Re_D. The agreement between the experiment and predictions for the low turbulence test cases help provide confidence in the experimental method.

Uncertainty Estimates. Uncertainties in the Nusselt number, Reynolds number and turbulence quantities were estimated using the root sum square method described by Moffat [25]. The uncertainty interval in the measurement of the Nusselt number is estimated to be less than +/- 6%. However, the uncertainty between runs is estimated to be +/- 3%. The uncertainty in the baseline value of Nusselt number used is estimated to be +/-2% due to the uncertainty in the stagnation region velocity gradient. The uncertainty in the heated to adiabatic-wall temperature difference was estimated to be +/- 0.2 °C. The uncertainty in the reported Reynolds number is estimated to be +/- 2%. The uncertainty in the reported turbulence level is estimated to be +/- 3%. The experimental error in determining scale was calculated to be +/- 11%. All estimates of uncertainty are reported for a 95% confidence interval.

EXPERIMENTAL RESULTS

A primary objective of the present investigation has been to significantly expand the parameter range for stagnation region heat transfer in order to span the relevant parameter space for current and future gas turbines. A second objective has been to test whether or not the trend toward large diameter leading edge designs will affect how turbulence influences stagnation region heat transfer. Ames and Moffat [10] developed the TRL parameter based on results of Hunt's analysis of turbulence approaching a 2-D bluff bodies. Hunt's analysis as well as Britter, Hunt, and Mumford's [7] data supported the concept that relatively small scale eddies are intensified in the strain field of a stagnation region. This intensification of turbulence approaching a stagnation region combined with attenuation of turbulence with wall blocking led Ames and Moffat to their TRL parameter $\{Tu\ (D/Lu)^{1/3}\ Re_D^{5/12}\}$. **Figure 7** presents some stagnation heat transfer data with turbulent augmentation from cylinders in cross flow, vane leading edge regions, and pin fins [5, 10-14]. The data show 80 independent points from 6 different studies with all but four points collecting within +/- 7% of the simple correlation.

$$Nu/Nu_0 = 1 + 0.04 * TRL \qquad (4)$$

However, in spite of these encouraging results, the two key objectives of this study, expanding the parameter space and understanding the impact of larger leading edges, have not been met. Earlier, Radomsky and Thole [26] published heat transfer distributions on a vane cascade with a very large leading edge diameter. They [27] also published turbulence measurements for the study. The stagnation region heat transfer augmentation for their high turbulence run was 55% above their laminar case but was overpredicted by 15% using the TRL correlation. Also, Van Fossen and Bunker's [16] stagnation region measurement for the DLN combustor at a 28% turbulence intensity was overpredicted by 12 percent. These two significant deviations from the TRL model for (a) a very large leading edge and (b) at a very high turbulence level, imply that the objectives of this present study are very relevant to the prediction of stagnation region heat transfer.

Stagnation Region Heat Transfer. This present data set extends the parameter range for stagnation region heat transfer to combinations of Reynolds numbers and turbulence levels which exceed values encountered in modern gas turbines. Heat transfer measurements for the six turbulence conditions outlined in **Table 1** have been taken at four nominal approach velocities ranging from 2.5 m/s to 20 m/s for the smaller (0.1016 m) and larger diameter (0.4064 m) cylindrical leading edge test surfaces. Heat transfer data sets were acquired using the smaller leading edge test surface over a diameter Reynolds number range of 15,600 to 125,000. Heat transfer data were acquired using the larger leading edge test surface over a Reynolds number range of 62,500 to 500,000. These data are presented in terms of the ratio of measured to baseline Nusselt number as a function of the TRL parameter in **Figure 8**. The baseline value for Nusselt number was given as $Nu_{0D}/Re_D^{0.5} = 0.873$ for the 0.1016 m diameter cylinder and $Nu_{0D}/Re_D^{0.5} = 1.002$ for the 0.4064 m cylinder as described in the baseline heat transfer section. These data extend the TRL parameter range from about 20 to over 50. The big leading edge cylinder data appear to begin dropping away from the simple TRL correlation given by equation (4) past a TRL of around 10. At the largest TRL value the measured heat transfer augmentation is only about 52% of the value estimated by equation (4). This large difference indicates the physics of the intensification of turbulence in the presence of a leading edge strain field has changed for this larger leading edge and to an extent by the smaller one as well. The impact of a rapidly strained flow on turbulence as suggested by Hunt [6] and measured by Britter, Hunt, and Mumford [7] may no longer be fully applicable to large diameter stagnation regions. The leading edge strain rate (dU/dx = 3.63 Vapp/D) is substantially lower than values expected for more conventional vane leading edge diameters. Ames [11] suggested that along a pressure surface of a vane, laminar heat transfer augmentation appears scale on $\{Tu\ (C/Lu)^{1/3}\ Re_C^{1/3}\}$. This parameter is similar to the effective laminar heat transfer augmentation scaling proposed by Dullenkopf and Mayle [17] for relatively large scale turbulence compared to the stagnation boundary layer thickness. In spite of the strong acceleration along a vane pressure surface, Ames found no evidence of intensification of turbulence taking place similar to the stagnation region.

Downstream Heat Transfer. Each leading edge cylinder has a constant radius leading edge over the first +/- 30° of the surface. Afterwards the surface has an increasing and continuously varying radius to allow the flow to smoothly accelerate downstream to the exit velocity as shown in **Figure 4**. Midline heat transfer distributions were acquired at the same time that the stagnation heat transfer measurements were taken. Heat transfer distributions for the 0.1016 m diameter leading edge test surface are presented in **Figure 9** for an approach velocity Reynolds number of 62,500. The heat transfer falls off rapidly from the peak at the stagnation line. The small grid placed 32 mesh lengths upstream shows high augmentation in the stagnation region but comparatively lower augmentation in the downstream region. The variation in augmentation from the stagnation region to the downstream region before transition clearly suggests that there is an intensification of turbulence near the stagnation point. This variation between leading edge and downstream heat transfer augmentation is also seen at the higher turbulence levels, although this difference is not as apparent due to early transition. Stagnation region augmentation levels range from 25% to 44% for the higher turbulence levels. In each case early transition is apparent downstream. The location of transition approximately correlates on turbulence intensity, although the aero-combustor with spool condition has a slightly higher turbulence intensity than the near grids but a very slightly delayed transition. Note that the peak velocity on the downstream heat transfer surface is only about 1.75 times the approach velocity.

Nusselt number distributions are also shown for the 0.1016 m diameter leading edge test surface in **Figure 10** for an approach velocity Reynolds number of 125,000. The heat transfer falls off rapidly at the leading edge. Similarly to **Figure 9**, the augmentation in the leading edge region is clearly higher than along the downstream surface. However, at the higher Reynolds number of this comparison, transition has moved upstream and the region of laminar augmentation downstream from the leading edge is shorter. The order of transition appears to be consistent with the lower Reynolds number comparison. Stagnation region augmentation levels range from 30% to 54% for the elevated turbulence levels for this condition.

Heat transfer distributions for the 0.4064 m diameter leading edge test surface have both similarities and differences to the 0.1016 m cylinder surface. Nusselt number distributions are presented for the 250,000 Reynolds number in **Figure 11**. The larger cylinder shows the high heat transfer over the broader leading edge. The small grid condition with higher spacing shows increased augmentation in the leading edge compared with the downstream region. The higher turbulence cases show distributions with sharp peaks suggesting the influence of fluid straining on the turbulence and as a result, the augmentation is relatively local and short lived in nature. The cylindrical surface shows transitional behavior downstream that is very similar in location to **Figure 9** which nominally has the same approach velocity. The flow over the large cylinder naturally has a smaller velocity gradient on the cylindrical leading edge but reaches a higher velocity on the heat transfer test surface. The peak velocity on the downstream heat transfer surface is about 2.05 times the approach velocity. Heat transfer augmentation levels ranged from 44% to 87% for this Reynolds number condition.

Nusselt number distributions for the 500,000 Reynolds number cases for the 0.4064 m diameter leading edge surface are presented in **Figure 12**. In spite of having only a two to one increase from approach to downstream velocity, the turbulent heat transfer in the low acceleration regions is now noticeably higher than the stagnation region. The stagnation area has a local peak in heat transfer which was also evident at the higher turbulence levels for the 250,000 Reynolds number cases. This peak may be due to the local intensification of turbulence by the highest strain rates close to the stagnation point. Outside of this local peak, the heat transfer level stays reasonably constant and then transitions shortly after the acceleration begins to decrease. The small grid shows some decrease in the downstream heat transfer augmentation level. However, this change is not as apparent as at this Reynolds numbers compared with the other data sets. The augmentation levels for the large cylinder at elevated turbulence range from 60% to 110%. The absolute heat transfer levels of the 0.1016 m diameter leading edge averages 34% higher at the elevated turbulence levels with similar inlet conditions when compared to the 0.4064 m diameter leading edge. However, the absolute increase in the heat transfer coefficient is about 18% higher for the 0.4064 m diameter leading edge.

SUMMARY AND CONCLUSIONS

Heat transfer measurements have been acquired using two cylindrical leading edge test surfaces (D_1 = 0.4064 m, D_2 = 0.1016 m) over an eight to one range in approach velocities at six turbulent conditions. Augmentation levels ranged from 10% to 54% for the 0.1016 m diameter leading edge and 25% to 110% for the 0.4064 m leading edge. The new experimental data largely collected within a range of +/- 7% of each other but fell well off the simple linear TRL correlation suggested by Ames [11]. At lower leading edge Reynolds numbers augmentation levels in the region of the leading edge were significantly higher than laminar augmentation levels downstream. The Nusselt number distributions on the downstream surface also provide some useful transition data for a range of turbulence levels and Reynolds numbers and moderate levels of acceleration. The absolute levels of heat transfer augmentation for the larger diameter (0.4064 m) leading edge were found to be on average 18% higher than the 0.1016 m diameter leading edge. However, the absolute level of heat transfer on the 0.1016 m diameter leading edge was found to average 34% higher than the larger (0.4064 m diameter) leading edge. These present data are expected to represent a significant expansion of the parameter range for stagnation region heat transfer in terms of high Reynolds numbers combined with high levels of turbulence.

ACKNOWLEDGEMENTS

The authors would like to gratefully acknowledge the support from the University of North Dakota for the faculty seed grant which supported this work. The facility used in this project was funded with a seed grant from the North Dakota EPSCoR Program. In addition, the authors are indebted to the University of North Dakota for providing additional support and laboratory space.

REFERENCES

[1] Zapp, G.M., 1950, “The effect of turbulence on local heat transfer coefficients around a cylinder normal to an air stream,” Master’s Thesis, Oregon State College.

[2] Smith, M.C., and Kuethe, A.M., 1966, “Effects of turbulence on laminar skin friction and heat transfer,” Physics of Fluids, vol. 9, no. 12, pp. 2337.

[3] Kestin, J., and Wood, R.T., 1971, “The influence of turbulence on mass transfer from cylinders,” J. Heat Transfer, pp. 321.

[4] Lowery, G.W., and Vachon, R.I. 1975, “The effect of turbulence on heat transfer from heated cylinders,” Int. J. Heat Mass Transfer, vol. 18, pp. 1229.

[5] Mehendale, A.B., Han, J.C., and Ou, S., 1991, “Influence of high mainstream turbulence on leading edge heat transfer,” ASME J. Heat Transfer, vol. 113, pp. 843-850.

[6] Hunt, J.C.R., 1973, “A theory of turbulent flow round two-dimensional bluff bodies,” J. Fluid Mech., vol. 61, part 4, p. 625.

[7] Britter, R. E., Hunt, J.C.R., and Mumford, J.C., 1979, “The distortion of turbulence by a circular cylinder,” Journal of Fluid Mechanics, vol. 92.

[8] Rigby, D.L., and Van Fossen, G.J., 1991, “Increased heat transfer to a cylindrical leading edge due to spanwise variations in the freestream velocity,” AIAA-91-1739, AIAA 22nd Fluid Dynamics, Plasma Dynamics and Lasers Conference, Honolulu, Hawaii.

[9] Kestin, J., 1966, “The effect of free-stream turbulence on heat transfer rate,” Advances in Heat Transfer, 3rd Ed., By T.F. Irvine and J.P. Harnett, Academic Press, London.

[10] Ames, F.E., and Moffat, R.J., 1990, “Heat Transfer with High Intensity, Large Scale Turbulence: The Flat Plate Turbulent Boundary Layer and the Cylindrical Stagnation Point,” HMT-44 (Ph.D. Dissertation), Stanford University.

[11] Ames, F.E., 1997, “The influence of large scale, high intensity turbulence on vane heat transfer,” ASME Journal of Turbomachinery, vol. 119, pp. 23-30.

[12] Ames, F.E., Wang, C., and Barbot, P.A., 2003, “Measurement and prediction of the influence of catalytic and dry low NOx combustor turbulence on vane surface heat transfer,” ASME Journal of Turbomachinery, vol. 125, pp. 210-220.

[13] Ames, F.E., Argenziano, M., Wang, C., 2004, “Measurement and prediction of heat transfer distributions on an aft loaded vane subjected to the influence of catalytic and dry low NOx combustor turbulence,” ASME Journal of Turbomachinery, vol. 126, pp 139-149.

[14] Ames, F.E., Dvorak, L.A., and Morrow, M.J., 2005, “Turbulent Augmentation of Internal Convection off Pins in Staggered Pin Fin Arrays,” ASME Journal of Turbomachinery, vol 127, pp. 183-190.

[15] Van Fossen, G.J., Simoneau, R.J., and Ching, C.Y., 1995, “Influence of turbulence parameters, Reynolds number, and body shape on stagnation region heat transfer, ASME J. Heat Transfer, vol. 117, pp. 597-603.

[16] Van Fossen, G.J. and Bunker R.S., 2001, “Augmentation of stagnation region heat transfer due to turbulence from a DLN can combustor,” ASME J. Turbomachinery, vol. 123, pp. 140-146.

[17] Dullenkopf, K., and Mayle, R.E., 1995, “An account of free-stream turbulence length scale on laminar heat transfer,” ASME J. Turbomachinery, vol. 117, pp. 401-406.

[18] Oo, A.N., and Ching, C.Y., 2002, “Stagnation line heat transfer augmentation due to freestream vortical structures and vorticity,” ASME J. Heat Transfer, vol. 124, pp. 583-587.

[19] Nix, A.C., Diller, T.E., and Ng, W. F., 2007, “Experimental Measurements and Modeling of the Effects of Large-Scale Freestream Turbulence on Heat Transfer,” ASME J. Turbomach., vol. 129, pp. 542–550.

[20] Nix, A.C., Diller, T.E., 2005, “Experiments on the Physical Mechanism of Heat Transfer Augmentation by Freestream Turbulence at a Cylinder Stagnation Point, GT-2005-68616.

[21] Gifford, A.R., Diller, T.E., and Vlachos, P.P., 2011, “The Physical Mechanism of Heat Transfer Augmentation in Stagnation Flow Subject to Freestream Turbulence,” ASME J. Heat Transfer, vol. 133, 021901-1-11.

[22] Bae, S., Lele, S.K., and Sung, H.G., 2002, “The influence of inflow disturbances on stagnation region heat transfer,” ASME J. Heat Transfer, vol. 122, pp. 258-265.

[23] Kays, W.M., Crawford, M.E, and Weigand, B.,, 2005, ***Convective Heat and Mass Transfer***, 4th Ed., McGraw-Hill, NY.

[24] Zukauskas, A., Ziugzda, J., 1985, ***Heat Transfer of a Cylinder in Crossflow,*** Hemisphere Publishing Corporation, NY.

[25] Moffat, R.J., 1988, “Describing the uncertainties in experimental results,” Experimental Thermal and Fluid Science, vol. 1., pp. 3-17.
[26] Radomsky, R, and Thole, K. A., 2002, “Detailed Boundary Layer Measurements on a Turbine Stator Vane at Elevated Freestream Turbulence Levels,” International Journal of Heat and Fluid Flow, v 23, n 2, p 137-147.
[27] Radomsky, R, and Thole, K. A., 2000, "Highly Turbulent Flowfield Measurements Around a Stator Vane," ASME Journal of Turbomachinery, **122**, pp. 255-262.

	Tu	U (m/s)	Λ_X (cm)	Lu (cm)	ε (m^2/s^3)
low turbulence	0.0069	4.96	8.12	127.0	0.00005
[LT]	0.0076	10.43	5.02	154.5	0.00035
	0.0060	18.71	3.58	15.5	0.0144
small grid	0.0297	2.33	1.69	3.38	0.015
[SGF]	0.0327	4.73	2.30	2.88	0.193
X/M = 29.6	0.0323	9.45	2.14	2.82	1.51
	0.0311	19.29	2.34	2.94	11.06
small grid	0.0945	2.44	1.29	1.49	1.24
[SGN]	0.0931	4.76	1.44	1.62	8.10
X/M = 7.7	0.0904	9.66	1.63	1.79	55.9
	0.0902	18.68	1.65	2.04	350.6
grid	0.0821	4.77	2.00	3.27	2.70
[Grid]	0.0861	10.19	2.04	3.35	29.8
X/M = 8.9	0.0884	19.27	2.35	3.53	206.8
combustor	0.0915	5.11	5.08	9.03	1.67
with spool	0.0950	9.74	4.61	8.81	13.23
[ACS]	0.0928	18.19	4.44	9.49	75.17
aeroderivative	0.1313	5.24	3.68	7.24	6.67
combustor	0.1402	9.32	3.52	6.36	51.5
[AC]	0.1339	18.39	3.58	7.35	302.0

Table 1. Inlet turbulence conditions generated for the present study

Medium Leading Edge (D = 0.1016 m)				
$Nu_D/ReD^{.5}$	0.861	0.851	0.838	0.823
Re_D	127,034	62,510	31,461	15,481
Large Leading Edge (D = 0.4064 m)				
$Nu_D/ReD^{.5}$	1.123	1.052	1.018	1.020
Re_D	491,590	244,344	121,396	60,818

Table 2. Low turbulence stagnation region $Nu/Re_D^{0.5}$ values as a function of Reynolds number and leading edge diameter.

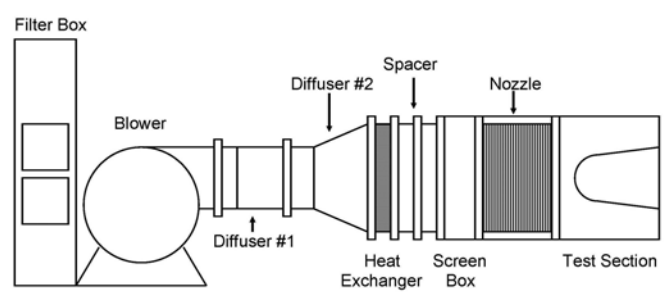

Figure 1. Schematic of Low Speed Wind Tunnel with Cylindrical Test Section

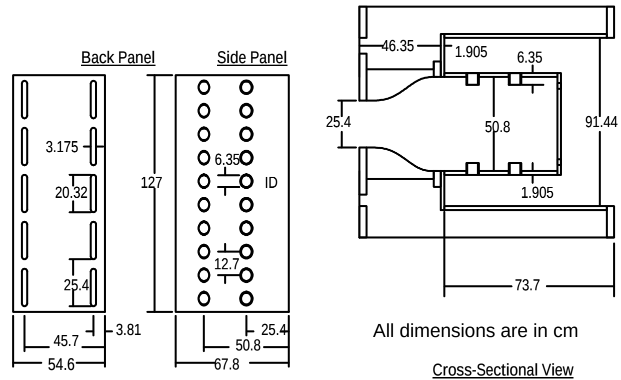

Figure 2. Schematic of model aero-combustor turbulence generator

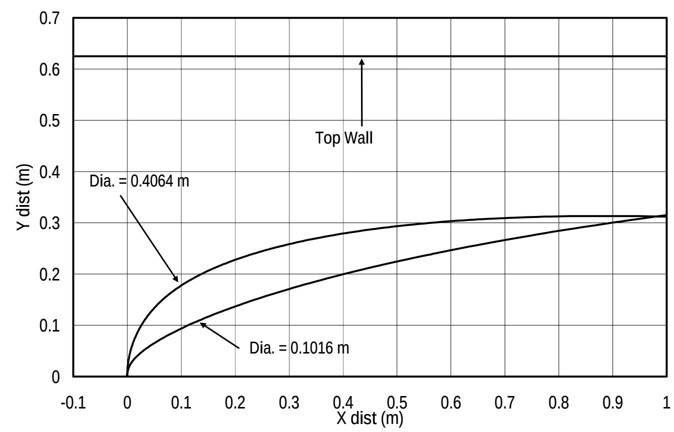

Figure 3. Geometries of the 0.1016 m and 0.4064 m diameter cylinders.

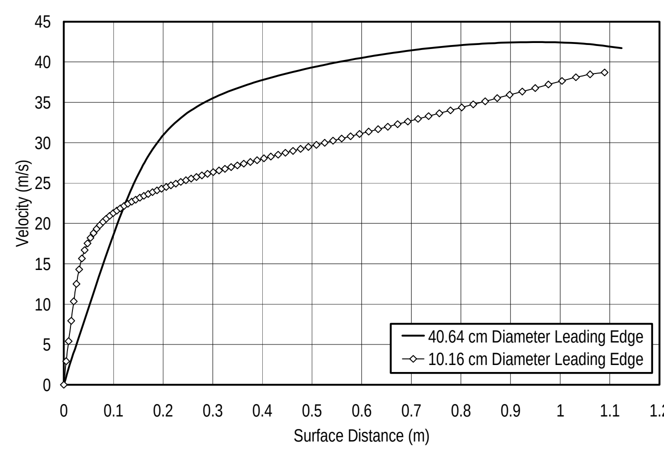

Figure 4. Calculated surface velocity distributions over 0.1016 m and 0.4064 m diameter leading edge cylinders.

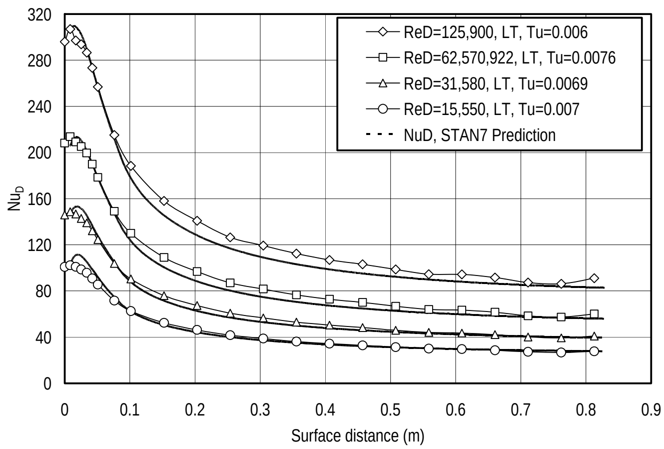

Figure 5. Comparison of experimental Nusselt number distributions for low turbulence condition with STAN7 predictions for smaller (0.1016 m) cylinder and afterbody.

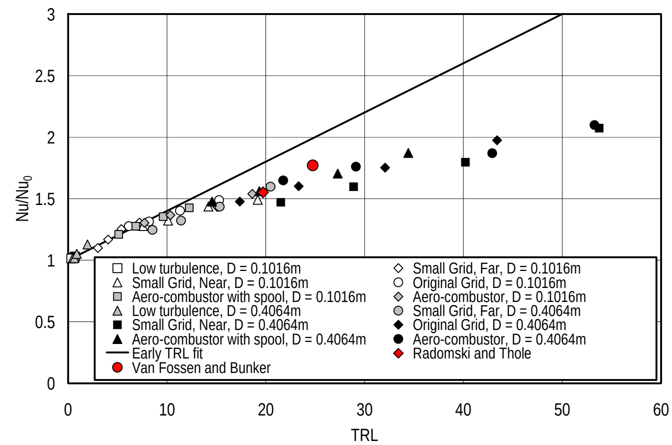

Figure 8. Nusselt number versus TRL parameter for smaller (0.1016 m) and larger (0.4064 m) cylindrical leading edge test surfaces.

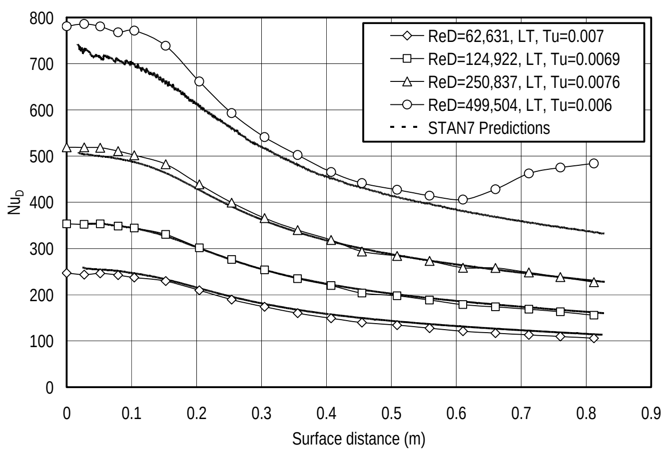

Figure 6. Comparison of experimental Nusselt number distributions for low turbulence condition with STAN7 predictions for larger (0.4064 m) cylinder and afterbody.

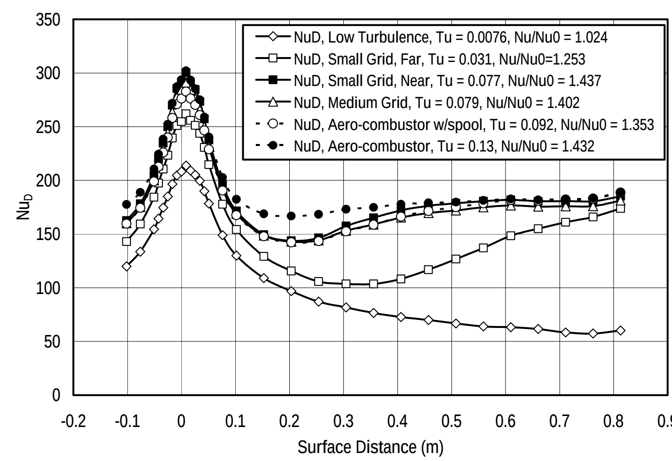

Figure 9. Nusselt number distribution on 0.1016 m diameter leading edge test surface for Re_D = 62,500 based on approach velocity comparing the influence of turbulence.

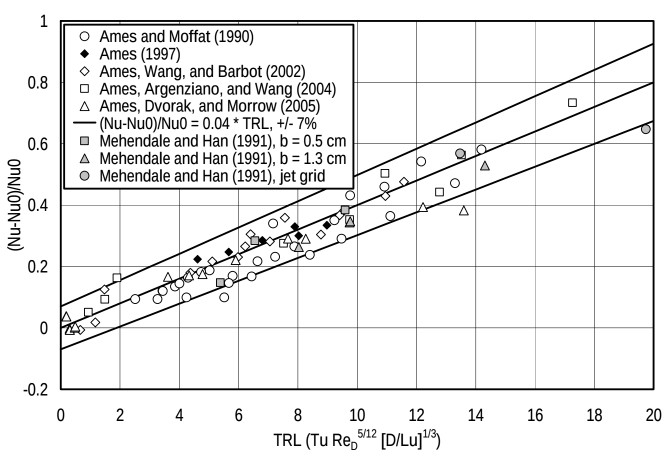

Figure 7. Correlation of the fractional increase in heat transfer versus the TRL parameter.

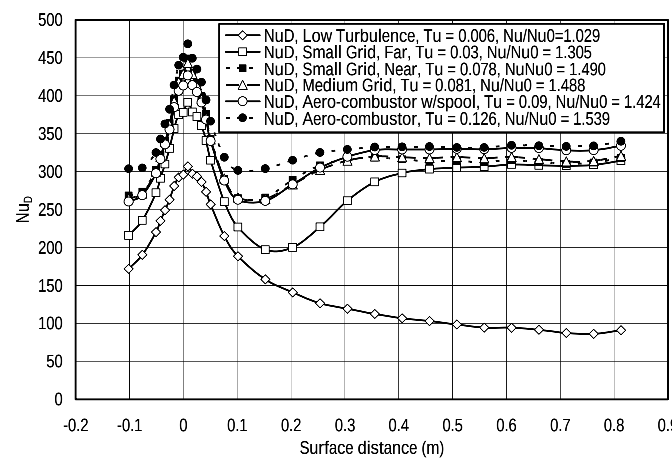

Figure 10. Nusselt number distribution on 0.1016 m diameter leading edge test surface, Re_D = 125,000 based on approach velocity comparing the influence of turbulence.

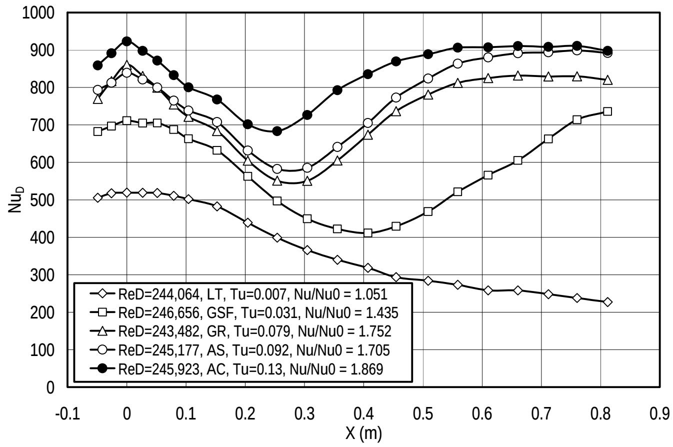

Figure 11. Nusselt number distribution on 0.4064 m diameter leading edge test surface, Re_D = 250,000 based on approach velocity comparing the influence of turbulence.

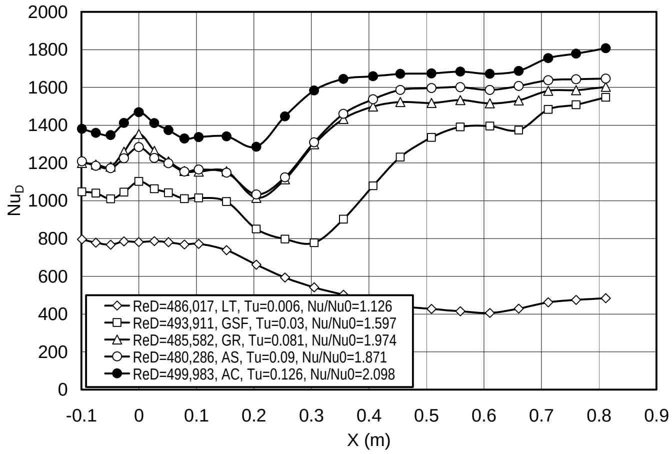

Figure 12. Nusselt number distribution on 0.4064 m diameter leading edge test surface, Re_D = 500,000 based on approach velocity comparing the influence of turbulence.

